

Deep Learning-Based Discrete Calibrated Survival Prediction

Patrick Fuhlert, Anne Ernst, Esther Dietrich, Fabian Westhaeusser, Karin Kloiber, Stefan Bonn

*Institute of Medical Systems Biology, Center for Biomedical AI (bAlome), Center for Molecular Neurobiology (ZMNH)
University Medical Center Hamburg-Eppendorf, Hamburg, Germany*

Abstract—Deep neural networks for survival prediction outperform classical approaches in discrimination, which is the ordering of patients according to their time-of-event. Conversely, classical approaches like the Cox Proportional Hazards model display much better calibration, the correct temporal prediction of events of the underlying distribution. Especially in the medical domain, where it is critical to predict the survival of a single patient, both discrimination and calibration are important performance metrics. Here we present Discrete Calibrated Survival (DCS), a novel deep neural network for discriminated and calibrated survival prediction that outperforms competing survival models in discrimination on three medical datasets, while achieving best calibration among all discrete time models. The enhanced performance of DCS can be attributed to two novel features, the variable temporal output node spacing and the novel loss term that optimizes the use of uncensored and censored patient data. We believe that DCS is an important step towards clinical application of deep-learning-based survival prediction with state-of-the-art discrimination and good calibration.

Index Terms—deep learning, discrimination, calibration, survival analysis, patient records, personalized medicine, clinical decision support, electronic health record

I. INTRODUCTION

Survival analysis or, in more general terms, time-to-event analysis, is a branch of statistics that analyses lifetimes of individuals or populations regarding a particular event (e.g. death) and infers what determines the underlying distributions [1]. In biomedical statistics, longitudinal patient data is analyzed to predict, for instance, the impact of a specific treatment on patient survival. This population-level analysis can determine which (groups of) patients benefit most from a given treatment and which prognostic features might be responsible for this. Classical statistics-based approaches for survival analysis include Kaplan-Meier (KM) survival curve analysis [2] and the Cox Proportional Hazards model (CoxPH) [3]. While KM analysis can be used to compare different patient groups characterized by one or more properties, the CoxPH model computes the relative risk of an event with respect to a reference population, on the basis of patient features or diagnostic results. Both approaches account for the characteristic right-censoring of patients, which refers to the fact that patients drop out due to unidentified reasons during the study. The use of this partial information of censored individuals distinguishes survival analysis from regression problems [4]. Other forms of censoring are rarely encountered in medical patient data, wherefore we focus on right-censored data in this study. The predictive performance of

survival models is commonly evaluated with the Concordance Index (C-index) and Cumulative-Dynamic AUROC (CDAUC), which are measures of discrimination that assess the correct ranking of predicted risks. While discrimination quantifies if a model predicts the correct order of events, it does not take into account if the predicted event occurs at the correct time. Especially in a clinical setting however, the correct prediction of the event time is of high relevance for the patient and medical practitioner, as it guides their decision making. The correct temporal prediction of an event can be measured by the calibration of a model, for example the Distributional Divergence for Calibration (DDC) [5]. Recent work concentrates on the development of deep learning-based (DL) algorithms for survival prediction, including models that produce a continuous time output like DeepSurv [6] and CoxTime [7]. Recent DL approaches such as DRSA [8] focus on the prediction of risk at discrete time points. While these discrete DL models reach state-of-the-art discrimination performance, they disregard model calibration, which makes them of limited value for medical survival prediction. To address this shortcoming, Kamran *et al.* developed a discrete DL model that focuses on model calibration [9]. In this work we present **Discrete Calibrated Survival (DCS)**, a survival model that extends the work of DRSA and Kamran to reach state-of-the-art discrimination while being well calibrated. We show that DCS outperforms five competing survival models, including DRSA and Kamran, in discrimination on three public medical tabular datasets, while achieving the best overall calibration for all discrete-time models. The performance gain in discrimination (CDAUC of 0.657 on SUPPORT, 0.773 on METABRIC, 0.832 on FLCHAIN) of DCS can be attributed to two novel ideas. First, DCS features a modified DRSA architecture that allows for variable temporal output node spacing in time. Best results were obtained with quantile spacing that ensures a uniform distribution of censoring and real events per discrete time step during model training. Second, DCS features a novel loss term that optimizes the use of uncensored and censored patient data to boost discrimination performance. This work uses the following structure. It starts with an overview of survival analysis and related work in section II, followed by section III that shows our experimental setup. Afterwards, the results are presented in section IV including comparisons to our baselines.

II. THEORY

A. Survival Analysis

Survival analysis focuses on the correct prediction of a future event, for instance the death of a patient or the relapse of a disease. While for some patients the event of interest might be recorded, other patients might leave a given study at any point in time without actually experiencing the event, giving rise to uncensored and (right-) censored patient data, respectively. Let $z_i = \min(t_i, c_i)$ be the time where an individual is either censored (c_i) or experiences the event of interest (t_i) (Fig. 1). From here on, let d_i denote the binary event indicator for each individual i : $d_i = \mathbb{1}_{z_i=t_i}$.

B. Models

This section describes current state-of-the-art survival prediction models that we compare to in this work and introduces our new DCS model.

1) *CoxPH*: The classical approach for survival analysis is the CoxPH model [3]. It finds the parameters that best reproduce the time-ordering of the individual events by fitting a logistic regression model that is based on the *Proportional Hazards Assumption* (that can be checked using Schoenfeld Residuals [10]) and assumes *linear* and *independent* covariates. The features of each individual are linearly combined $g\beta(\mathbf{x}_i) = \beta^T \mathbf{x}_i$ and optimized using a partial likelihood approach. Afterwards, the regression model is joined with a baseline hazard that is equal for the whole population. By design, predicted survival curves have the same shape for all individuals (effectively discarding individual temporal information) of the population and only differ in a unique parametric scaling factor per patient that depends on the individual's input features.

2) *DeepSurv*: Since neural networks rather learn the underlying functional dependencies than assuming them, they permit the discovery of non-linear dependencies between the survival model's covariates [6]. DeepSurv retains the partial likelihood function, such that all predicted survival curves have the same shape with a different scaling factor, just as in the CoxPH model. In other words, the encoding of the predictor $g(\mathbf{x}_i)$ is calculated by a neural network that obtains the covariate information as input.

3) *CoxTime*: Similar to DeepSurv, CoxTime [7] uses a discriminative partial likelihood objective function, but introduces a time-variant degree of freedom in the survival curves by feeding the desired prediction time into the network as an

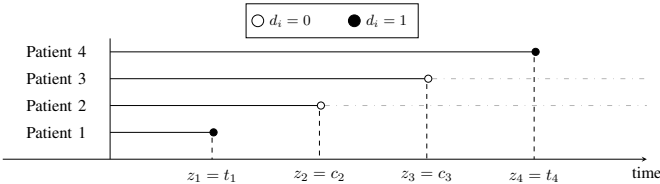


Fig. 1. In time-to-event analysis, individuals either experience the event ($d_i = 1$) or are censored ($d_i = 0$) at some point in time (z_i).

additional input. This relaxes the proportionality constraint from the model to allow for potentially crossing survival curves that violate the proportional hazards assumption.

4) *DRSA*: The algorithm abandons the log-likelihood loss and instead computes the conditional probabilities of the event over time [8]. In particular, the architecture includes a Recurrent Neural Network (RNN) which is designed to utilize the sequential characteristic of the survival curve. It evaluates the hazard rate predictions at the discrete output time steps before and at the event time for each individual. Furthermore, the index $l \in \{1, \dots, L\}$ of the current time step is an additional input feature to the encoder. Since the model predicts hazard rates h_l for each discrete time point t_l , the survival curve prediction for individual i is obtained by

$$\hat{S}(t_l | x_i) = \prod_{j=1}^l (1 - h_j). \quad (1)$$

5) *Kamran*: The survival prediction model of Kamran [9] utilizes the architecture of DRSA but implements a novel loss function that emphasized proper model calibration. The first term, \mathcal{L}_{RPS} , uses the **R**ank **P**robability **S**core. Uncensored individuals contribute with a mean-squared-error loss that compares the individual's estimated survival function to a prediction that drops from one to zero at the discretized event time z_i at the discrete output time point with index l_i . Moreover, censored individuals ($d_i = 0$) only contribute up to the point of censoring z_i and are compared to a prediction of one:

$$\mathcal{L}_{\text{RPS}} = \sum_{i=1}^n \left[d_i \cdot \sum_{l=1}^{L_i} \left(\hat{S}(t_l | \mathbf{x}_i) - \mathbb{1}_{l < l_i} \right)^2 + (1 - d_i) \cdot \sum_{l=1}^{l_i} \left(\hat{S}(t_l | \mathbf{x}_i) - 1 \right)^2 \right]. \quad (2)$$

Here, $\hat{S}(t_l | \mathbf{x}_i)$ denotes the estimated survival curve at time t_l with the individual i 's feature vector \mathbf{x}_i , and the corresponding index l_i of the discrete event time z_i . The second loss term $\mathcal{L}_{\text{kernel}}$ emphasizes proper discrimination of the model by penalizing the wrong ordering of two *uncensored* individuals

$$\mathcal{L}_{\text{kernel}} = \sum_{i=1}^n \sum_{j=1}^n A_{i,j} \cdot \exp \left(-\frac{1}{\sigma} \left(\hat{S}(z_i | \mathbf{x}_j) - \hat{S}(z_i | \mathbf{x}_i) \right) \right) \quad (3)$$

where every non-zero entry of $A_{i,j} = \mathbb{1}_{(i \neq j, d_i = d_j = 1, z_i < z_j)}$ corresponds to one comparison of two non-censored individuals i and j . Since $z_i < z_j$, the prediction $\hat{S}(z_i | \mathbf{x}_i)$ should be smaller than $\hat{S}(z_i | \mathbf{x}_j)$ to minimize this loss for all comparisons. Note that large values for σ will emphasize the spreading of predictions for uncensored pairs. Lastly, the two loss parts are combined with a hyperparameter λ for weighting to

$$\mathcal{L}_{\text{Kamran}} = \mathcal{L}_{\text{RPS}} + \lambda \mathcal{L}_{\text{kernel}}. \quad (4)$$

Kamran uses a discrete output node per month and \mathcal{L}_{RPS} is evaluated on the survival curve $\hat{S}(t | x_i)$ directly, instead of the hazard rates h_l as in DRSA.

6) *DCS*: Our new DCS model can be divided into an encoder, decoder, and aggregation part and predicts a survival curve $\hat{S}(t|\mathbf{x})$ given a feature vector \mathbf{x} , as illustrated in Fig. 2. **Model Architecture** - The basic architecture of DCS is an extension and modification of DRSA that we will highlight in this section. **Encoder**: In contrast to DRSA, the encoder network does not append the index l to the encoded feature vector \mathbf{x} since it did not improve our results. This leads to a simplified encoding that is the same for every predicted time-step. Compared to DRSA, we also allow multiple fully connected encoder layers. **Decoder**: The LSTM structure is extended to allow a skip connection that concatenates the original encoder output to the LSTM output for every timestep. Additionally, we introduce a bidirectional LSTM to maximize the usage of temporal information forwards and backwards in time. **Aggregation**: To combine the LSTM's output for each timestep t_l to a scalar hazard rate h_l , a fully connected network of one or more layers is used instead of only a single layer. **Loss Function** - DCS features a modified kernel loss term $\tilde{\mathcal{L}}_{\text{kernel}}$ to optimize the use of both censored and uncensored patient data for better discriminative performance. The original kernel loss (3) is extended to not only include event-to-event (EE), but also event-to-censoring (EC) comparisons of two individuals i and j where the individual j with the latter event time ($z_i < z_j$) is censored ($d_j = 0$). This modification increases the number of comparable training data pairs to boost discriminative performance. In more detail, we relax the condition ($d_i = d_j = 1, z_i < z_j$) of the masking matrix A in (3), that only includes EE comparisons, to our new condition ($d_i = 1, z_i < z_j$) that adds EC comparisons in the novel masking matrix B , resulting in the following kernel loss:

$$\tilde{\mathcal{L}}_{\text{kernel}} = \sum_{i=1}^n \sum_{j=1}^n B_{i,j} \cdot \exp \left[-\frac{1}{\sigma} \left(\hat{S}(z_i | \mathbf{x}_j) - \hat{S}(z_i | \mathbf{x}_i) \right) \right], \quad (5)$$

where $B_{i,j} = \mathbb{1}_{(i \neq j, d_i=1, z_i < z_j)}$. This increases the maximum number of comparisons for e.g. the SUPPORT dataset from 1.81×10^7 to 3.41×10^7 , a factor of $F = 1.9$. The factor F depends on the censoring rate and the censoring distribution of each dataset as shown in Tab. I. Moreover, this work analyzes the relation between the censoring rate and the number of comparisons for a dataset in detail in the supplemental material. The second DCS loss term is identical to the RPS calibration loss of Kamran (2). We introduced a normalization step for the two independent losses to achieve better orthogonalization of the hyperparameters batch size and λ . Without this normalization, the batch size would influence the choice of λ since the weighting of the loss terms depends on the number of individuals n and the number of output nodes L that might be included in the hyperparameter search space. While $\mathcal{L}_{\text{RPS}} \in \mathcal{R}^{n \times L}$ is normalized by its width L and height n , $\mathcal{L}_{\text{kernel}} \in \mathcal{R}^{n \times n}$ is a sparse matrix that is normalized by the number of actual comparisons $n_{\text{comp}} = |B|$. This normalization step leads to our final objective function:

$$\mathcal{L}_{\text{ours}} = \frac{1}{nL} \mathcal{L}_{\text{RPS}} + \frac{\lambda}{n_{\text{comp}}} \tilde{\mathcal{L}}_{\text{kernel}} \quad (6)$$

Temporal Spacing of Predictions - Kamran and DRSA use equidistant temporal spacing (*linear spacing*) of survival predictions, such that every consecutive inference predicts the survival of a patient for e.g. another month. While equidistant temporal predictions are a natural choice, they might not be optimal for model learning given the training data distribution. To obtain a model with high-quality predictions for earlier as well as later time-points, we propose two alternative temporal output node spacings to get a more uniform distribution of events per time-point, as outlined in Fig. 3. Histograms for the other datasets in this work can be found in the supplemental material. As a medical motivation, one might argue that the difference between surviving 100 and 200 days should be more important than the difference between 1100 and 1200 days, thus motivating a *logarithmic spacing* of predictions. To enforce a strictly uniform distribution of training events per time-point, one can ensure that at each time-point an equal amount of individuals either experience the event or are censored, which we call *quantile spacing*.

C. Metrics

1) *Discrimination*: Discrimination quantifies if a model predicts the correct order of events, it does not scrutinize if the predicted event occurs at the correct time. An example for the usage of discrimination is an organ transplant waiting list, where the patient with the best survival estimate after transplantation is selected as the most suitable candidate. In this work we measure discrimination with the Time-Dependent

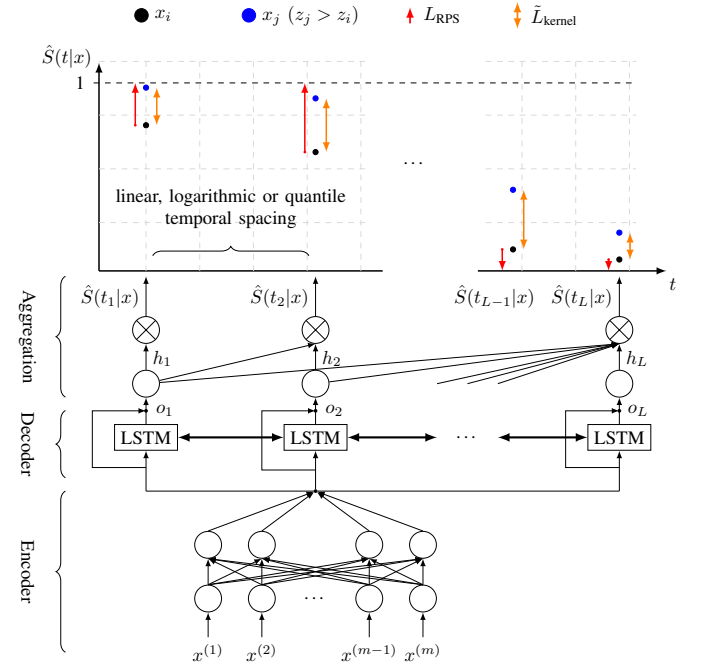


Fig. 2. Visualization of the DCS network architecture from individual features \mathbf{x} to the output of a survival curve prediction $\hat{S}(t|\mathbf{x})$. The red arrows indicate the \mathcal{L}_{RPS} loss, which minimizes the distance of the prediction to 1, before the event, and 0, after the event. The novel DCS $\tilde{\mathcal{L}}_{\text{kernel}}$ loss maximizes the distance between x_i and x_j , as shown in orange.

Concordance Index (C-index-td) [11] and the Cumulative-Dynamic AUROC (CDAUC) [12].

Time-Dependent Concordance Index - The C-index [13] is the most commonly used metric for discriminative performance of survival models. It is a generalization of the area under the ROC curve (AUC) [11] that evaluates the correct ordering of predictions compared to actual event times. Several models we evaluate allow crossing survival curve predictions (i.e. the order of individuals can change over time). To properly evaluate these time-dependent changes, we use the Time-Dependent Concordance Index (C-index-td) [11], which evaluates the C-index at the event times.

$$C^{td} = P(\hat{S}(z_i|x_i) < \hat{S}(z_j|x_j) \mid z_i < z_j, d_i = 1) \quad (7)$$

Cumulative-Dynamic AUROC (CDAUC) - To measure how well a model can distinguish individuals that experience an event before or at time $z_i \leq t$ from those that did not experience an event yet ($z_i > t$), a time dependent receiver operating characteristic curve (ROC) and the corresponding area under the curve can be defined as [14]:

$$AUC(t) = P(\hat{S}(t|x_i) < \hat{S}(t|x_j) \mid z_i \leq t, z_j > t) \quad (8)$$

To generate a scalar metric for the whole time span of the dataset, the $AUC(t)$ is weighted (by the KM estimate $\hat{S}(t)$) and integrated by the inverse probability of censoring:

$$CDAUC := \frac{1}{\hat{S}(\tau_1) - \hat{S}(\tau_2)} \int_{\tau_1}^{\tau_2} AUC(t) d\hat{S}(t). \quad (9)$$

As opposed to the C-index, the CDAUC is a proper scoring method. No prediction model has a higher discriminative value than the data generating process itself [14].

2) *Calibration*: A patient or medical practitioner might be interested if the prediction reflects the true underlying survival distribution. A relapse time of 2 or 20 years will make a difference for the selected therapy, independent of the ordering of other patients. We measure calibration with the DDC [9]. *Distributional Divergence for Calibration (DDC)* - The estimated survival for each individual at their event time $\hat{S}(z_i|x_i)$ is mapped into 10 equally sized bins \mathcal{B} in the unit interval as shown in [5]. For DDC, the KL-Divergence [15] is calculated between the relative frequency P of the observed intervals compared to the uniform distribution $Q(b) = 0.1$:

$$DDC(P||Q) = \sum_{b \in \mathcal{B}} P(b) \log \left(\frac{P(b)}{Q(b)} \right) \quad (10)$$

TABLE I

Number of comparisons $|A|$ and $|B|$ for each analyzed dataset that corresponds to the number of non-zero entries in A and B respectively. Also included is the number of patients, censoring rate and the factor of more comparisons $F = |B|/|A|$.

	patients	censoring rate	$ A $	$ B $	F
SUPPORT	8873	32 %	1.81×10^7	3.41×10^7	1.9
METABRIC	1904	42 %	6.08×10^5	1.25×10^6	2.0
FLCHAIN	7874	72 %	2.35×10^6	1.34×10^7	5.7

III. EXPERIMENTS

A. Datasets

We evaluated the presented models on the following three public medical EHR datasets to analyze the discrimination and calibration performance. The basic and relevant properties of those datasets are depicted in Tab. II.

SUPPORT [16] - The Study to Understand Prognoses and Preferences for Outcomes and Risks of Treatments provides information about 8873 seriously ill hospitalized adults with 14 features (demographic, observational, and lab data). The endpoint is the time of death of a patient.

METABRIC [17] - This dataset from the Molecular Taxonomy of Breast Cancer International Consortium is the smallest analyzed dataset of this work. 1904 patients with 9 features (demographic, molecular drivers and therapies) are given to predict long-term clinical outcome of breast cancer.

FLCHAIN [18] - This study analyzes the impact of free light chain and creatinine blood serum levels. They also include basic demographic information in their analysis to predict patient mortality.

B. Implementation

In our experiments we use the CoxPH model from `lifelines` [19], `DeepSurv` and `CoxTime` from `pycox` [7]. The DRSA, Kamran and our DCS models were self-implemented in Tensorflow 2.5.0 and Python 3.8.7. The implementation uses external implementations of the C-index-td (`pycox`) and CDAUC (`scikit-survival` [20]). The Distributional Divergence for Calibration was self-implemented. For automated hyperparameter tuning we used `scikit-learn` [21] wrappers for all models, preprocessing

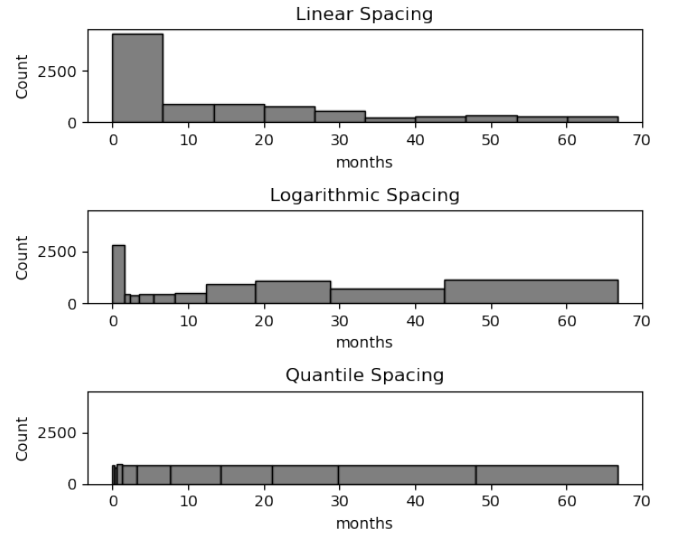


Fig. 3. Histograms of the number of events per temporal prediction on SUPPORT. Ten predictions in time are made with linear, logarithmic and quantile temporal spacing.

workflows, and datasets. Our code with all datasets, baseline models, pipelines, hyperparameter tuning, and metrics can be found in our repository at <https://github.com/imsb-uke/dcsurv>.

C. Data Processing

The dataset features are standardized and imputed, where required. Numerical features are standardized to a mean of zero and a standard deviation of one. To impute missing values, we use *median imputation* for numerical and *most frequent imputation* for categorical features. Categorical features are one-hot encoded. For the SUPPORT dataset, zeros in some continuous features like heart rate or respiration rate were also treated as missing values and imputed accordingly. To evaluate the continuous and discrete time models as fair as possible, all estimations are projected on the same time-steps. We chose the training set event and censoring times for evaluation. For this purpose, all model predictions were interpolated linearly between their temporal output node time points.

D. Hyperparameter Tuning

For hyperparameter tuning and performance evaluation we split the data into 80% training and 20% test data stratified by the event indicator. The test data was only used during the final evaluation of the model performances. A detailed description of the hyperparameter tuning and the best parameters for each model can be found in the supplements.

IV. RESULTS

We compare the discrimination and calibration performance of CoxPH, DeepSurv, CoxTime, DRSA, Kamran, and three variants of DCS with linear, logarithmic, and quantile output node spacing on the SUPPORT, METABRIC, and FLCHAIN test data. To obtain variance estimations for the model performance, we use 10-fold bootstrapping and report the ‘mean \pm standard deviation’. In the evaluation we focus on three scenarios, the overall best model per metric, the performance gains achieved by DCS’s novel kernel loss and our novel **linear**, **logarithmic** and **quantile** spacing approaches. Overall, DCS models reach best discriminative performance for both the C-index-td (Tab. III) and the CDAUC (Tab. IV). More specifically, the DCS model with quantile output node spacing (DCS-quant) displays top performance in four out of six comparisons. DCS-quant shows the best C-index-td on the SUPPORT (0.628) and METABRIC (0.698) datasets,

while DCS-linear reaches first place on the FLCHAIN dataset (0.803) (Tab. III). Regarding the CDAUC, DCS-quant exhibits top performance on the METABRIC (0.773) and FLCHAIN (0.832) datasets, while the DCS-log model is best on the SUPPORT data (0.658) (Tab. IV). These results suggest that both, the novel kernel loss (5) and new output spacing, increase discriminative performance as measured with the C-index-td and CDAUC, robustly outperforming all competing models. To specifically understand the influence of the modified kernel loss (5) on discriminative performance, we compare DCS-linear to Kamran. For all three datasets, DCS-linear outperforms Kamran in the C-index-td (SUPPORT 0.628 vs. 0.610, METABRIC 0.694 vs. 0.668, FLCHAIN 0.803 vs. 0.786). Similarly, DCS-linear surpasses Kamran in the CDAUC on METABRIC (0.730 vs. 0.727) and FLCHAIN (0.813 vs. 0.807), while it is slightly worse on the SUPPORT (0.641 vs. 0.652) data. Lastly, it is interesting to observe that the continuous time models CoxPH, DeepSurv, and CoxTime outperform the discrete DRSA and Kamran models in the C-index-td. Continuous time models reach the best calibration as measured by DDC, while DCS-quant reaches the best calibration performance of all discrete time models (Tab. V). For instance, CoxTime features a slightly lower (better) DDC as compared to DCS-quant across all datasets (SUPPORT 0.066 vs. 0.007, METABRIC 0.027 vs. 0.009, FLCHAIN 0.021 vs. 0.006). Among the discrete time models, our DCS-quant shows superior performance compared to DRSA on all datasets (SUPPORT 0.066 vs. 0.193, METABRIC 0.027 vs. 0.296, FLCHAIN 0.021 vs. 0.050) and to Kamran on two out of three datasets (SUPPORT (0.066 vs. 0.139, METABRIC 0.027 vs. 0.065, FLCHAIN 0.021 vs. 0.006). These results provide strong evidence that (quantile) output node spacing can boost both, calibration and discrimination performance of survival models.

TABLE III
Test set results for C-index-td (\uparrow).

		SUPPORT	METABRIC	FLCHAIN
cont.	CoxPH	0.594 \pm 0.009	0.638 \pm 0.020	0.798 \pm 0.007
	DeepSurv	0.604 \pm 0.012	0.679 \pm 0.014	0.795 \pm 0.014
	CoxTime	0.612 \pm 0.007	0.675 \pm 0.019	0.790 \pm 0.010
disc.	DRSA	0.598 \pm 0.006	0.661 \pm 0.019	0.792 \pm 0.018
	Kamran	0.610 \pm 0.006	0.668 \pm 0.023	0.786 \pm 0.013
ours	DCS-linear	0.623 \pm 0.009	0.694 \pm 0.018	0.803 \pm 0.011
	DCS-log	0.623 \pm 0.009	0.674 \pm 0.018	0.792 \pm 0.008
	DCS-quant	0.628 \pm 0.009	0.698 \pm 0.019	0.794 \pm 0.015

V. CONCLUSION

In this work we present a novel DL-based survival model, DCS, with state-of-the-art discrimination and good calibration. Two novel features that are introduced in DCS seem to be primarily responsible for this performance increase. First, we introduce an extension of the Kamran $\mathcal{L}_{\text{kernel}}$ loss [9], which uses event-to-event and event-to-censoring pairs during training to boost discrimination. We show that our $\hat{\mathcal{L}}_{\text{kernel}}$ increases the number of comparisons for the analyzed datasets by a factor of approximately 2 to 6 as compared to the original

TABLE II

Number of patients, number of features, censoring rate, percent of missing data, median survival time and ratio of covariates that violate the proportional hazards assumption (non-prop.) for each dataset.

	SUPPORT	METABRIC	FLCHAIN
patients	8873	1904	7874
features	14	9	8
censoring rate	32 %	42 %	72 %
missing data	0.1 %	0 %	1.7 %
median surv.	57 days	85 months	71 months
non-prop.	79 %	56 %	25 %

TABLE IV
Test set results for CDAUC (\uparrow).

		SUPPORT	METABRIC	FLCHAIN
cont.	CoxPH	0.619 \pm 0.013	0.686 \pm 0.028	0.797 \pm 0.019
	DeepSurv	0.634 \pm 0.016	0.700 \pm 0.032	0.800 \pm 0.016
	CoxTime	0.647 \pm 0.010	0.747 \pm 0.020	0.799 \pm 0.012
disc.	DRSA	0.613 \pm 0.008	0.685 \pm 0.029	0.814 \pm 0.014
	Kamran	0.652 \pm 0.018	0.727 \pm 0.024	0.807 \pm 0.018
ours	DCS-linear	0.641 \pm 0.012	0.730 \pm 0.021	0.813 \pm 0.017
	DCS-log	0.658 \pm 0.011	0.716 \pm 0.028	0.824 \pm 0.015
	DCS-quant	0.657 \pm 0.012	0.773 \pm 0.023	0.832 \pm 0.017

TABLE V
Test set results for DDC (\downarrow).

		SUPPORT	METABRIC	FLCHAIN
cont.	CoxPH	0.009 \pm 0.003	0.021 \pm 0.007	0.001 \pm 0.000
	DeepSurv	0.010 \pm 0.003	0.017 \pm 0.006	0.003 \pm 0.002
	CoxTime	0.007 \pm 0.002	0.009 \pm 0.004	0.006 \pm 0.001
disc.	DRSA	0.193 \pm 0.009	0.296 \pm 0.024	0.050 \pm 0.004
	Kamran	0.139 \pm 0.006	0.065 \pm 0.013	0.006 \pm 0.002
ours	DCS-linear	0.141 \pm 0.013	0.138 \pm 0.010	0.012 \pm 0.002
	DCS-log	0.055 \pm 0.005	0.071 \pm 0.006	0.035 \pm 0.004
	DCS-quant	0.066 \pm 0.006	0.027 \pm 0.008	0.021 \pm 0.004

implementation by Kamran. These additional comparisons improve the discriminative performance regarding C-index-td as well as CDAUC on the three analyzed datasets. Second, we introduce three temporal output node spacings (linear, logarithmic, and quantile spacing) to increase the model discrimination and calibration. Overall, the quantile approach (DCS-quant) provides the best discriminative performance on the three datasets we investigated. DCS-quant also reaches the best calibration for discrete time models (DRSA and Kamran) for two of three datasets. While DCS-quant shows best calibration for discrete time models, it is slightly worse than the calibration of the continuous time models (CoxPH, DeepSurv, and CoxTime). A reason for the good calibration of continuous time models, at the cost of inferior discrimination, might be that the time-dependent baseline hazard already defines a reasonable population wide survival estimate. This could suggest that continuous models might suffer from bad calibration on datasets with time-dependent underlying baseline hazards. Our results also indicate that the C-index-td might not be the best metric to evaluate discriminative performance in survival prediction. Whereas the C-index-td for the FLCHAIN dataset yields very similar values for all models inspected, the CDAUC shows clear differences in model performance. In the end, DCS provides researchers with a model that reaches best-of-breed discrimination and good calibration and might pave the way towards future clinical application of deep-learning-based survival prediction.

ACKNOWLEDGEMENTS

PF and AE were supported by the KFO 306 and LFF-FV 78 grants. ED received funding from the SFB 1192 project B8. FW was supported by the UKE M3I grant and SB by

the UKE R3 reduction of animal testing grant. KK received funding from the UKE deanery.

REFERENCES

- [1] J. P. Klein and M. L. Moeschberger, *Survival analysis: techniques for censored and truncated data*. Springer, 2003, vol. 2.
- [2] E. L. Kaplan and P. Meier, "Nonparametric estimation from incomplete observations," *Journal of the American Statistical Association*, vol. 53, no. 282, pp. 457–481, 1958.
- [3] D. R. Cox, "Regression models and life-tables," *Journal of the Royal Statistical Society: Series B (Methodological)*, vol. 34, no. 2, pp. 187–202, 1972.
- [4] Z. Meng *et al.*, "A multi-task kernel learning algorithm for survival analysis," in *Pacific-Asia Conference on Knowledge Discovery and Data Mining*. Springer, 2021, pp. 298–311.
- [5] H. Haider *et al.*, "Effective ways to build and evaluate individual survival distributions," *J. Mach. Learn. Res.*, vol. 21, no. 85, pp. 1–63, 2020.
- [6] J. L. Katzman *et al.*, "DeepSurv: Personalized treatment recommender system using a Cox proportional hazards deep neural network," *BMC Medical Research Methodology*, vol. 18, no. 1, pp. 1–12, feb 2018. [Online]. Available: <https://link.springer.com/articles/10.1186/s12874-018-0482-1>
- [7] H. Kvamme *et al.*, "Time-to-event prediction with neural networks and Cox Regression," *Journal of Machine Learning Research*, vol. 20, pp. 1–30, 2019. [Online]. Available: <http://jmlr.org/papers/v20/18-424.html>.
- [8] K. Ren *et al.*, "Deep recurrent survival analysis," *33rd AAAI Conference on Artificial Intelligence, AAAI 2019, 31st Innovative Applications of Artificial Intelligence Conference, IAAI 2019 and the 9th AAAI Symposium on Educational Advances in Artificial Intelligence, EAAI 2019*, pp. 4798–4805, sep 2019. [Online]. Available: <http://arxiv.org/abs/1809.02403>
- [9] F. Kamran and J. Wiens, "Estimating Calibrated Individualized Survival Curves with Deep Learning," *The Thirty-Fifth AAAI Conference on Artificial Intelligence*, vol. 35, no. 1, pp. 240–248, 2021. [Online]. Available: <https://ojs.aaai.org/index.php/AAAI/article/view/16098>
- [10] S. Park and D. J. Hendry, "Reassessing schoenfeld residual tests of proportional hazards in political science event history analyses," *American Journal of Political Science*, vol. 59, no. 4, pp. 1072–1087, 2015.
- [11] L. Antolini *et al.*, "A time-dependent discrimination index for survival data," *Statistics in Medicine*, vol. 24, no. 24, pp. 3927–3944, dec 2005. [Online]. Available: <http://doi.wiley.com/10.1002/sim.2427>
- [12] H. Uno *et al.*, "Evaluating prediction rules for t-year survivors with censored regression models," *Journal of the American Statistical Association*, vol. 102, no. 478, pp. 527–537, jun 2007. [Online]. Available: <https://www.tandfonline.com/doi/abs/10.1198/016214507000000149>
- [13] F. E. Harrell *et al.*, "Evaluating the Yield of Medical Tests," *JAMA*, vol. 247, no. 18, pp. 2543–2546, may 1982. [Online]. Available: <https://jamanetwork.com/journals/jama/fullarticle/372568>
- [14] P. Blanche *et al.*, "The c-index is not proper for the evaluation of t-year predicted risks," *Biostatistics*, vol. 20, no. 2, pp. 347–357, 2019.
- [15] S. Kullback and R. A. Leibler, "On Information and Sufficiency," <https://doi.org/10.1214/aoms/1177729694>, vol. 22, no. 1, pp. 79–86, mar 1951. [Online]. Available: <https://projecteuclid.org/journals/annals-of-mathematical-statistics/volume-22/issue-1/On-Information-and-Sufficiency/10.1214/aoms/1177729694.full>
- [16] W. A. Knaus *et al.*, "The SUPPORT prognostic model. Objective estimates of survival for seriously ill hospitalized adults," *Annals of Internal Medicine*, vol. 122, no. 3, pp. 191–203, 1995.
- [17] C. Curtis *et al.*, "The genomic and transcriptomic architecture of 2,000 breast tumours reveals novel subgroups," *Nature*, vol. 486, no. 7403, pp. 346–352, 2012.
- [18] T. M. Therneau, *A Package for Survival Analysis in R*, 2022, r package version 3.3-1. [Online]. Available: <https://CRAN.R-project.org/package=survival>
- [19] C. Davidson-Pilon *et al.*, *CamDavidsonPilon/lifelines: v0.25.7*, Dec. 2020. [Online]. Available: <https://doi.org/10.5281/zenodo.4313838>
- [20] S. Pölsterl, "scikit-survival: A library for time-to-event analysis built on top of scikit-learn," *Journal of Machine Learning Research*, vol. 21, no. 212, pp. 1–6, 2020. [Online]. Available: <http://jmlr.org/papers/v21/20-729.html>
- [21] F. Pedregosa *et al.*, "Scikit-learn: Machine learning in Python," *Journal of Machine Learning Research*, vol. 12, pp. 2825–2830, 2011.

Deep Learning-Based Discrete Calibrated Survival Prediction

Supplemental Material

Patrick Fuhler, Anne Ernst, Esther Dietrich, Fabian Westhaeusser, Karin Kloiber, Stefan Bonn
 Institute of Medical Systems Biology, Center for Biomedical AI (bAlome), Center for Molecular Neurobiology (ZMNH)
 University Medical Center Hamburg-Eppendorf, Hamburg, Germany

S-1. ESTIMATING THE NUMBER OF COMPARISONS FOR C-INDEX-TD AND NEWLY PROPOSED LOSS

Suppose a dataset D with n individuals and a censoring rate of $c \in [0, 1)$. When drawing two individuals i and j from D at random, under the assumption that censoring is uniformly distributed throughout the observed event time, the chance of picking a pair (i, j) that is comparable regarding the C-index-td (??) or $\tilde{\mathcal{L}}_{\text{kernel}}$ (??) (EE or EC pair) is

$$P(\text{comp}_{\text{new}}) = P(d_i = 1, d_j = 1, z_i < z_j) + P(d_i = 1, d_j = 0, z_i < z_j) \quad (\text{S-1})$$

and can be estimated by using the censoring rate c of randomly drawing a censored individual from the dataset. Under the assumption that, when picking a random pair (i, j) , the corresponding event times are equally distributed, the probability that the first event time z_i is smaller than z_j is assumed as $P(z_i < z_j) = 0.5$. Firstly, the relative frequency of drawing only EE pairs which corresponds to the number of comparisons in (??) can be estimated as

$$P(\text{comp}_{\text{old}}) = P(d_i = 1, d_j = 1, z_i < z_j) = (1 - c)^2 / 2. \quad (\text{S-2})$$

Furthermore, we add the comparisons where the former event time is uncensored and the latter event time is censored as

$$P(d_i = 1, d_j = 0, z_i < z_j) = c(1 - c) / 2. \quad (\text{S-3})$$

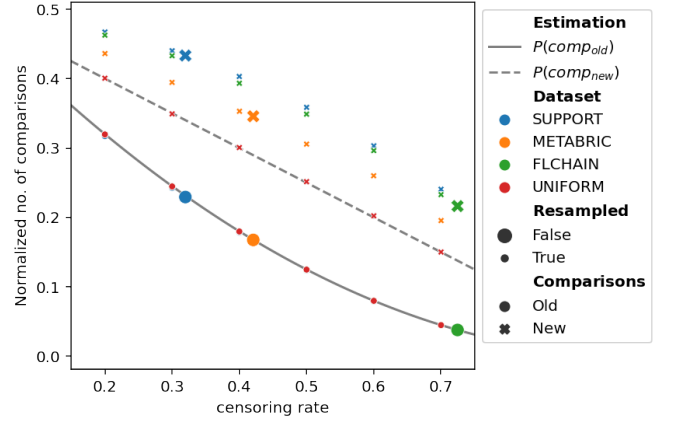
Combining (S-2) and (S-3) leads to the final estimation for the new number of comparisons

$$P(\text{comp}_{\text{new}}) = (1 - c)^2 / 2 + c(1 - c) / 2 = (1 - c) / 2. \quad (\text{S-4})$$

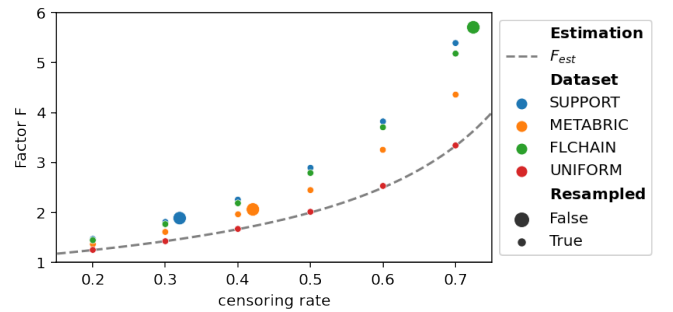
Since the old $\mathcal{L}_{\text{kernel}}$ (??) only compared all uncensored pairs for i and j that led to $P(\text{comp}_{\text{old}}) = (1 - c)^2$, the factor F of more comparisons can be estimated from (S-2) and (S-4) as

$$F_{\text{est}} = P(\text{comp}_{\text{new}}) / P(\text{comp}_{\text{old}}) = 1 / (1 - c). \quad (\text{S-5})$$

This estimation can now be compared to the observed number of comparisons from Tab. ?? in Fig. S-1. It is shown that our estimation closely matches the number of old comparisons for all datasets as well as the number of new comparisons for



(a) Number of normalized comparisons n_{comp}/n^2 and estimations (S-2, S-4) over the censoring rate. Old comparisons are depicted with "o" while new comparisons are shown with an "x".



(b) Factor F (S-5) of more comparisons over the censoring rate.

Fig. S-1. Observed (markers) and estimated (lines) number of comparisons over the censoring rate for the analyzed datasets. We also include a synthetic dataset ('uniform') in red with a uniform censoring distribution. To generate additional datapoints, the datasets are resampled to match predefined censoring rates that are depicted with smaller markers.

the synthetically created new "uniform" dataset. It is shown that, for higher censoring rates, the factor F suggests that our approach allows for significantly more comparisons on datasets with high censoring rates (e.g. 70 % censoring leads to approximately 3 to 6 times more comparisons). Also notice that the observed factor F is even higher than predicted for the real-world datasets which indicates that the assumption of a uniform censoring distribution is not met.

S-2. HYPERPARAMETER TUNING

This work utilizes a bayesian hyperparameter search with `scikit-optimize`. The data was split into 80% train and 20% test data stratified by the event indicator. Afterwards, 5-fold cross-validation on the training set was performed with 100 iterations to find the best hyperparameters. The CDAUC was chosen as the optimization criterion. The best model was then retrained on the complete training dataset with the previously found best hyperparameters. We used a fixed batch size of 50 and trained all models for 100 epochs. To avoid overfitting during training, we added early stopping with a patience of 10 epochs and included a 20 % dropout rate.

The tunable hyperparameters of the DeepSurv and CoxTime models were the number of layers and nodes per layer of the networks. CoxPH did not have any tunable hyperparameters. In DRSA, the loss weighting parameter α was also included as a hyperparameter.

All models that are based on the DRSA architecture, namely DRSA, Kamran, and DCS, share the following tunable hyperparameters. The *encoder* part represents the dense network structure before the LSTM, the *decoder* the LSTM structure itself and *aggregation* the dense network that converts each of the decoder outputs into a scalar value. Each subnetwork’s number of layers and number of nodes were hyperparameter tuned. Moreover, we introduce the observation window T_{\max} that corresponds to the maximum survival time in months for each training dataset. We then use the data-driven approach of defining the total number of output nodes L as a hyperparameter based on T_{\max} , such that $L \in \{.25, .5, 1, 2\} \cdot T_{\max}$. Note that this approach only sets the number of output nodes L of the network and is independent of the temporal spacing (linear, logarithmic or quantile) of those nodes. Furthermore, instead of fixing the loss weighting parameter λ to 1 as in the original Kamran model, it is also included together with σ (??) in the hyperparameter search space for Kamran and all DCS models.

Table S-1 shows the best hyperparameters per model for each dataset. For all discrete-time models, the optimal network architectures tend to be rather shallow. In some cases, some parts of the architecture, namely encoder, decoder, or aggregation are dismissed. Notice that DeepSurv and CoxTime almost always have best performance with shallow neural networks – usually with one hidden layer, even though the search space included up to five. For the aggregation part of the network, one fully connected layer is necessary to map the decoder’s output to a single hazard rate h_i . In our approach, we allow additional fully connected aggregation layers for a deeper model architecture. We also analyzed the influence of the total number of output nodes in the hyperparameter tuning. Here we can see incoherent results that might depend on the dataset as well as the temporal spacing of output nodes. In some cases, increasing the number of output nodes yields the best results (e.g. DCS-linear, DCS-log on SUPPORT and METABRIC), in others (e.g. DCS-quant on SUPPORT and METABRIC) less

total output nodes L were selected.

S-3. EVENT HISTOGRAMS OF OTHER DATASETS

Histograms of the number of events per temporal prediction for the METABRIC and FLCHAIN datasets are shown in Fig. S-3.

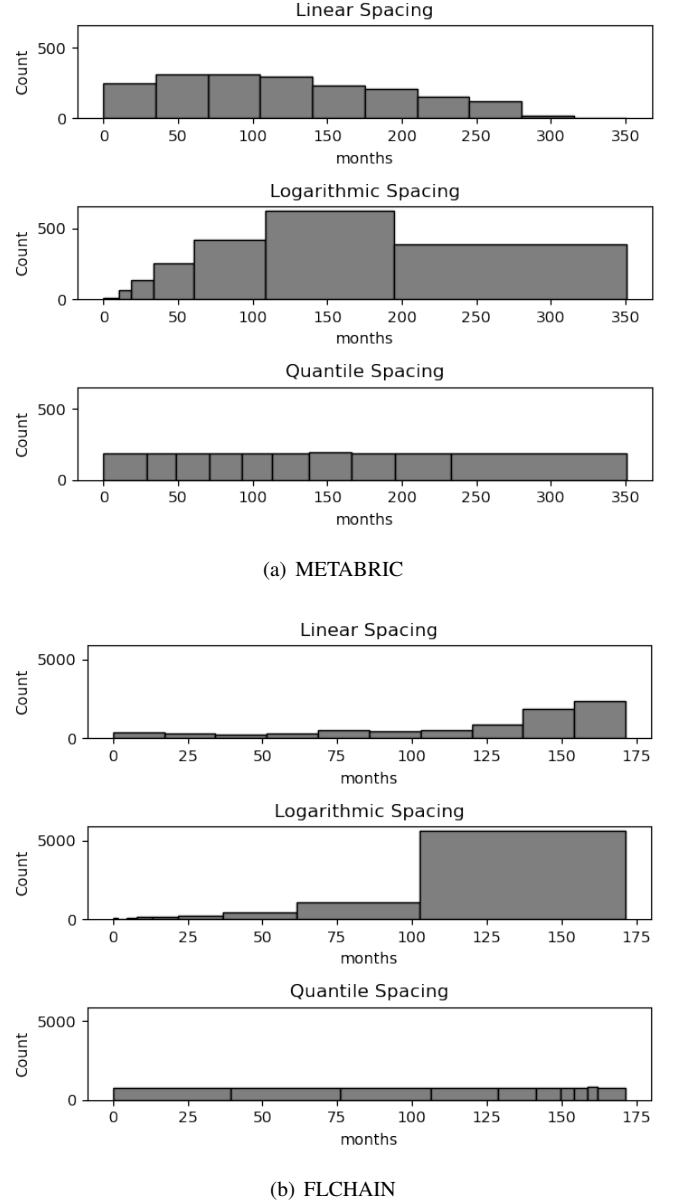


Fig. S-2. Histograms of the number of events per temporal prediction on METABRIC and FLCHAIN. Ten buckets in time are made with linear, logarithmic and quantile temporal spacing.

TABLE S-1
Best hyperparameters for all analyzed datasets and the presented models.

SUPPORT	DeepSurv	CoxTime	DRSA	Kamran	DCS-linear	DCS-log	DCS-quant
encoder_num_layers	1	1	0	0	1	2	2
encoder_nodes_per_layer	64	32	-	-	32	128	64
decoder_num_layers			1	1	1	0	1
decoder_nodes_per_layer			128	32	32	-	64
decoder_bidirectional					0	-	1
decoder_use_lstm_skip					0	-	0
aggregation_num_layers				1	1	1	2
additional_aggregation_nodes_per_layer				-	-	-	32
output_grid_num_nodes			280	67	140	140	35
α			0.36				
λ				2.00	0.85	0.25	2.00
σ				1.08	1.55	2.00	1.00
METABRIC	DeepSurv	CoxTime	DRSA	Kamran	DCS-linear	DCS-log	DCS-quant
encoder_num_layers	1	1	0	0	2	1	0
encoder_nodes_per_layer	8	8	-	-	128	64	-
decoder_num_layers			1	1	2	1	2
decoder_nodes_per_layer			128	64	64	64	32
decoder_bidirectional					0	1	0
decoder_use_lstm_skip					1	1	0
aggregation_num_layers				1	2	1	1
additional_aggregation_nodes_per_layer				-	32	-	-
output_grid_num_nodes			350	350	700	350	60
α			0.03				
λ				1.94	1.19	1.08	0.25
σ				1.63	0.25	1.45	2.00
FLCHAIN	DeepSurv	CoxTime	DRSA	Kamran	DCS-linear	DCS-log	DCS-quant
encoder_num_layers	5	1	1	0	1	0	1
encoder_nodes_per_layer	64	8	64	-	64	-	64
decoder_num_layers			1	1	1	1	0
decoder_nodes_per_layer			16	32	64	128	-
decoder_bidirectional					1	1	-
decoder_use_lstm_skip					1	0	-
aggregation_num_layers				1	1	1	1
additional_aggregation_nodes_per_layer				-	-	-	-
output_grid_num_nodes			42	171	125	42	85
α			0.39				
λ				1.34	2.00	0.67	1.13
σ				0.34	1.00	0.46	0.73